JOURNAL OF GEOPHYSICAL RESEARCH, VOL. 115, A03305, doi:10.1029/2009JA014562, 2010

Penetration of magnetospheric electric fields to the equator and their effects on the low-latitude ionosphere during intense geomagnetic storms

B. Veenadhari,[1,2] S. Alex,[1] T. Kikuchi,[2] A. Shinbori,[2] Rajesh Singh,[1] and E. Chandrasekhar[3]

Received 18 June 2009; revised 10 October 2009; accepted 16 October 2009; published 17 March 2010.

[1] The penetration of magnetospheric electric fields to the magnetic equator has been investigated for two intense magnetic storms that occurred on 31 March 2001 and 6 November 2001. The digital ground magnetic data from equatorial station Tirunelveli (TIR, 0.17°S geomagnetic latitude (GML)) and low-latitude station Alibag (ABG, 10.17°N GML) have been used to identify the storm time electrojet index, EEJ(Dis), which is the difference of the magnetic field variations between TIR and ABG after removing the quiet day variations. The appearance of enhanced *DP* 2 currents and counterelectrojets (CEJ) during the main and recovery phases of the magnetic storms is possibly due to prompt penetration of electric fields from the high latitudes. These signatures can be interpreted as a clear indicator of the eastward and westward electric fields at the equator. The observed results suggest that the magnitude of the equatorial ionospheric currents driven by the penetrating electric fields is very sensitive to ionospheric conductivity (which depends on local time). Moreover, the intensity of the *DP* 2 currents started decreasing during the end of the main phase of the storm despite the large negative southward IMF Bz, indicating the dominance of a well-developed shielding electric field for 1 h. As an effect of penetrating electric fields at the equator, the equatorial ionization anomaly is enhanced during the main phase (because of strong eastward electric field) and is inhibited or reduced due to the strong CEJ (because of westward electric field) during the recovery phase.

Citation: Veenadhari, B., S. Alex, T. Kikuchi, A. Shinbori, R. Singh, and E. Chandrasekhar (2010), Penetration of magnetospheric electric fields to the equator and their effects on the low-latitude ionosphere during intense geomagnetic storms, *J. Geophys. Res.*, *115*, A03305, doi:10.1029/2009JA014562.

1. Introduction

[2] It is well known that the two-cell convection (*DP* 2 currents) in the high latitudes driven by a reconnection process [e.g., *Dungey*, 1961] between the Earth's magnetic field and southward interplanetary magnetic field (IMF) manifests negative and positive geomagnetic field variations in the morning and afternoon sectors, respectively. The geomagnetic field variations from high latitudes to the equator associated with the quasiperiodic *DP* 2 currents have one-to-one correspondence with the IMF variations [*Nishida et al.*, 1966; *Nishida*, 1968]. *Kikuchi et al.* [1996] demonstrated that the large-scale convection electric fields that drive the *DP* 2 currents accompanied with region 1 (R1) field-aligned currents (FACs) can instantaneously penetrate from high latitudes to the equator by means of the zeroth-order transverse magnetic (TM_0) mode waves in the Earth's ionosphere waveguide. The TM_0 mode propagates in the waveguide at the speed of light, accompanying electric currents in the conducting ionosphere [*Kikuchi et al.*, 1978; *Kikuchi and Araki*, 1979]. *Wilson et al.* [2001] pointed out that enhanced *DP* 2 currents were observed in the middle latitudes during a major geomagnetic storm, at the same time that a strong convection electric field was detected by the CRRES satellite, located in the equatorial region of the inner magnetosphere ($L < 5$). They also suggested that the storm time electric field is attributed to the development of ring current in the inner magnetosphere. In addition to the manifestation of *DP* 2 currents in the ionosphere, the enhanced convection electric field produces a partial ring current with strong dawn-dusk asymmetry in the inner magnetosphere. The partial ring current generates region 2 (R2) FACs and shielding electric field with an opposite direction to the convection electric field in the inner magnetosphere through some magnetosphere-ionosphere coupling processes [*Vasyliunas*, 1972; *Jaggi and Wolf*, 1973; *Southwood*, 1977; *Senior and Blanc*, 1984]. The shielding

[1]Indian Institute of Geomagnetism, Navi Mumbai, India.
[2]Solar-Terrestrial Environment Laboratory, Nagoya University, Nagoya, Japan.
[3]Department of Earth Sciences, Indian Institute of Technology, Mumbai, India.

0148-0227/10/2009JA014562

effect due to the dusk-to-dawn electric field persists for about 17–30 min as estimated by models [*Senior and Blanc*, 1984; *Peymirat et al.*, 2000] and magnetometer observations during substorms [*Somayajulu et al.*, 1987; *Kikuchi et al.*, 2000]. In the case when the R1 FACs and dawn-to-dusk electric field abruptly decrease because of the northward turning of the IMF, the dusk-to-dawn electric field is dominant in the inner magnetosphere [*Kelley et al.*, 1979]. This condition is called overshielding. The overshielding condition is determined by the competition between the R1 and R2 FACs with strong dependence on the IMF direction [*Rastogi and Patel*, 1975; *Gonzales et al.*, 1979; *Kobea et al.*, 2000]. The overshielding electric field also penetrates to the equator and produces negative variations of geomagnetic field at the daytime equator as counterelectrojets (CEJ) [*Kikuchi et al.*, 2008]. *Reddy et al.* [1979, 1981] detected a westward electric field caused by CEJ in the daytime equatorial ionosphere with VHF backscatter radar during a geomagnetic storm.

[3] *Huang et al.* [2005] suggested that the penetration of convection electric field to low latitudes persists for 2–3 h without the shielding during the main phase using Millstone Hill and Jicamarca incoherent scatter radar data. On the other hand, *Kikuchi et al.* [2008] pointed out that the convection electric field can be depressed from the middle latitudes to the equator during the late main phase when the shielding electric field significantly grows because of the development of the ring current in the inner magnetosphere. Furthermore, during the recovery phase caused by the reduction of southward IMF or northward turning IMF, the reversed electric field appears with a significant intensity of 2–3 mV/m in the inner magnetosphere [*Wygant et al.*, 1998], and at the same time significant reduction of the *H* component occurs at the equatorial region because of enhanced CEJ [*Rastogi*, 2004; *Kikuchi et al.*, 2008] associated with overshielding condition [*Huang et al.*, 2001]. However, the other important ionospheric disturbance dynamo electric fields, with time scales from a few to several hours, are driven by enhanced energy deposition into the high-latitude ionosphere [*Blanc and Richmond*, 1980]. The relatively fast (occurring about 2–3 h after major increase in convection) disturbance dynamo electric fields are probably due to dynamo action of fast traveling equatorward wind surges, and slow disturbances (occurring about 3–12 h later) are believed to be driven mostly by electrodynamic action of storm time enhanced winds [*Fejer et al.*, 2007, and references therein]. But their large spatial and temporal variability still remains unsolved [*Fejer*, 2002 and references therein]. But the time interval discussed in this paper is prior to the effect of the disturbance dynamo. The prompt penetration of the convection electric fields from high latitudes to equatorial latitudes during geomagnetic disturbances causes the *F* region plasma modifications and uplift of the ionosphere during daytime/nighttime with correspondence to the eastward and westward electric fields [*Tsurutani et al.*, 2004]. On the other hand, at low latitudes, the ionospheric positive storm phase during daytime was driven by enhanced meridional wind rather than the penetration of electric field [*Lu et al.*, 2008]. But a strong daytime eastward penetration electric field can strengthen the equatorial plasma fountain [e.g., *Hanson and Moffett*, 1966] to a super plasma fountain (which is a strong enhancement of the equatorial ionization anomaly (EIA)), which, in turn, can lead to strong positive ionospheric storms at low latitudes and midlatitudes [*Kelley et al.*, 2004]. Recently, the precondition of a super plasma fountain and evaluation of its effect on EIA have been studied using an ionospheric model [*Balan et al.*, 2009].

[4] The well-developed theoretical and model explanations of penetrating convection electric fields to the low latitudes and at the equator during intense geomagnetic storms have led to a substantial understanding, but there remain several unanswered questions: (1) How does the temporal and spatial variation of the penetrating electric fields last for an unexpectedly long lifetime under the overshielding condition [*Fejer*, 2002; *Huang et al.*, 2005]? (2) How does the delay time between the *DP* 2 currents and the development of ring current during the onset time of geomagnetic storms depend [*Kikuchi et al.*, 2008]? (3) What are the major roles of convection and overshielding electric fields on ionospheric dynamics, such as super plasma fountain effect and the formation of the EIA? Because of the lack of simultaneous observations of vertical electric field drifts from radar measurements and geomagnetic field observations from low and equatorial latitudes, the above problems have not been resolved so far. Also, penetrating electric fields during different local times other than noon and night are not well understood [*Tsurutani et al.*, 2008]. In this paper, an attempt is made to answer these questions by investigating temporal and spatial variations of the penetrating electric fields, equatorial *DP* 2 currents, and CEJ and associated changes in the ionospheric plasma at low latitudes and the equator during two intense magnetic storms. In particular, daytime *F* region ionospheric plasma response to strong eastward and westward electric fields is examined using ground geomagnetic field and ionosonde observations.

2. Data

[5] We have selected two intense geomagnetic storms that occurred on 31 March 2001 and 6 November 2001 during the solar cycle 23. The digital ground magnetic data with time resolution of 1 min are provided from Indian magnetic observatories Alibag (ABG, geographic latitude 18.62°N, geographic longitude 72.87°E; 10.17°N geomagnetic latitude (GML)) and equatorial station Tirunelveli (TIR, geographic latitude 8.7°N, geographic longitude 77.8°E; 0.17°S GML). The TIR station is convenient to monitor the equatorial electrojet (EEJ), while the ABG is located outside its influence. The simultaneous data obtained from these two stations are thus well suited for estimating the strength of the equatorial electrojet, particularly during the storm time conditions when the ground level magnetic variations receive contributions not only from the overhead currents in the ionospheric dynamo region but also from distant currents from magnetospheric sources. The geomagnetic field data obtained from ABG are used as a reference for calculation of equatorial *DP* 2 since it is located outside the equatorial electrojet and far from the high-latitude geomagnetic disturbances. However, wind-driven currents can also be an important factor in changing the magnitude of EEJ and CEJ, which is well explained using simulations with NCAR Thermosphere-Ionosphere-Electrodynamics-General Circulation Model (TIE-GCM) by *Fang et al.* [2008]. The EEJ

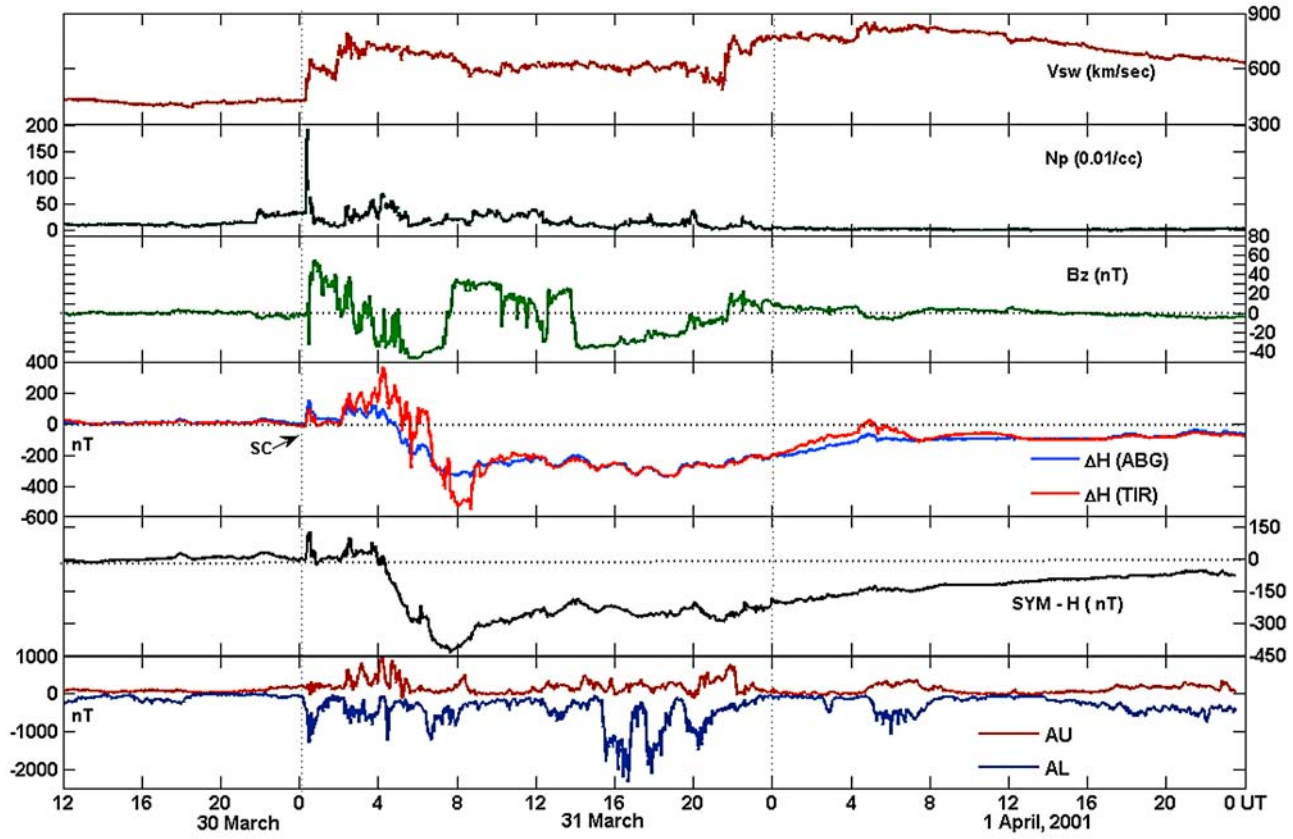

Figure 1. Magnetic storm of 31 March to 1 April 2001 with ΔH of TIR and ABG, *SYM-H* index, interplanetary magnetic field component (IMF Bz), solar wind velocity (Vsw), and proton density (Np) from ACE. On 31 March, the solar wind shock arrived at 0014 UT accompanied with a large increase in proton density. The SC occurred at 0015 UT on 31 March 2001 with a large decrease in IMF Bz. The main phase started after almost 3 h of SC. The local noon is at around 0600–0700 UT (1130–1230 LT), and local midnight is at around 1830–1930 UT (0000–0100 LT).

(Dis) index does not provide the information on storm time winds. To study the ionospheric *F* region response to the penetrating electric fields during the geomagnetic storms, the ionosonde data with time resolution of 15 min are used from the equatorial station Trivandrum (TRD, geographic latitude 8.48°N, geographic longitude 76.95°E; 0.31°S GML) and the near-equatorial station Vishakapatnam (VSK, geographic latitude 17.68°N, geographic longitude 83.32°E; 8.34°N GML). The data obtained from the low latitude stations at Ahmedabad (AHD, geographic latitude 23.03°N, geographic longitude 72.58°E; 14.01°N GML) and Delhi (DEL, geographic latitude 28.3°N, geographic longitude 77.01°E; 19.02°N GML), which are located almost at the crest of EIA, are also used in the present study. The solar wind and other interplanetary parameters are obtained from the Advanced Composition Explorer (ACE) spacecraft, positioned at about 224 R_E. The *SYM-H*, *AU*, and *AL* indices, which are good indicators of geomagnetic activity, are used to identify the maximum auroral eastward and westward electrojet currents associated with the enhanced two-cell convection, respectively. These geomagnetic indices are provided by the World Data Center, Kyoto, Japan. The polar cap potential index (PCN) is used to estimate the polar cap potential drop conditions during the magnetic storm period, which is taken from polar cap station Thule (THL, 85.22° corrected geomagnetic latitude (CGML)). The equatorial storm time electrojet index [*Alex et al.*, 1986] represented by EEJ(Dis) is calculated by the difference between ΔHsd (TIR) and ΔHsd (ABG), where ΔHsd refers to the difference between ΔH (storm day) and ΔH (quiet day) for each location. The baseline of ΔH corresponds to the nighttime value of the *H* component. We assume that the geomagnetic field variations in ΔH at ABG mainly consist of the effects of ring currents flowing in the inner magnetosphere. Since the *DP* 2 currents at low latitudes are smaller than those at the equator, EEJ(Dis) provides us a proxy index for electric field variations at the altitude of the ionosphere during the main and recovery phases of geomagnetic storms [*Veenadhari and Alex*, 2006].

3. Observations and Results

3.1. Geomagnetic Storm on 31 March 2001

[6] Figure 1 shows an overview of the ground geomagnetic variations in ΔH from ABG and TIR, *SYM-H*, and *AU* and *AL* indices, along with IMF Bz, solar wind velocity, and proton density during the intense geomagnetic storm of 31 March 2001. The time interval is 2.5 days from 30 March

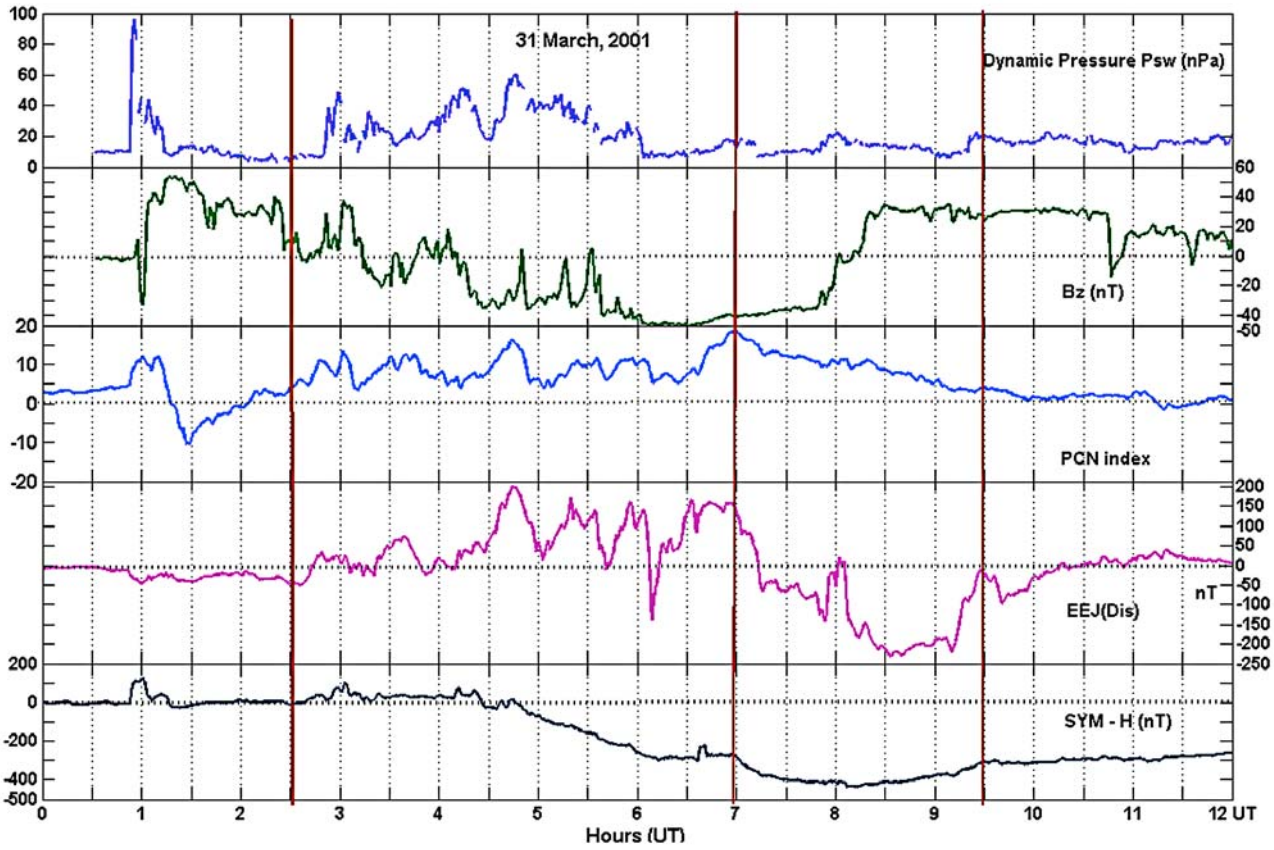

Figure 2. The dynamic pressure of solar wind (Psw), IMF Bz along with storm time electrojet index, EEJ(Dis), and PCN index are plotted from 0000 to 1200 UT for 31 March 2001 (the local noon corresponds to 0600–0700 UT (1130–1230 LT). The portion between the thick vertical lines indicates the strong *DP* 2 currents (EEJ) and counterelectrojet (CEJ) during the main and recovery phases of the magnetic storm on 31 March 2001 (see text).

1200 UT to the end of 1 April. Furthermore, the solar wind and IMF data were time-shifted by around 30 min on the basis of the comparison between geomagnetic field and IMF signatures. This geomagnetic storm is classified into one of the most intense magnetic storms of solar cycle 23. The large halo coronal mass ejection (CME) with X1.7 X-ray flare in the AR 9393 region occurred at 1015 UT on 29 March and led to the high-speed solar wind and strong southward IMF that are believed to be responsible for this storm [*Srivastava and Venkatakrishnan*, 2002]. This led to a shock at the Earth's magnetosphere, starting at about 0014 UT on 31 March 2001, after 38 h. The first shock passed through the ACE position at ~0022 UT on 31 March 2001. The sudden commencement (SC) occurred at 0051 UT on 31 March 2001 with maximum amplitudes of 96.4 nT and 149.8 nT at TIR and ABG, respectively. About 3 h after the arrival of the solar wind shock, the IMF gradually turned from northward to southward with the large intensity. The first long duration of the northward IMF led to the long initial phase of the geomagnetic storm after SC. The CME induced a very strong and prolonged period of southward IMF (Bz), reaching to less than −30 nT intermittently over a period of nearly 4 h from SC and reaching a minimum of nearly −50 nT at ~0630 UT. The strong southward IMF with a value of less than −30 nT, over a period of nearly 4 h, triggered very strong magnetospheric convection in the magnetosphere and the intense geomagnetic storm reaching a maximum of *SYM-H* ≈ −435 nT and also maximum decreases of the ΔH of TIR and ABG are about −500 nT and −350 nT, respectively, during the main phase. The southward IMF Bz caused the development of ring current in the inner magnetosphere, indicating a negative excursion of the *SYM-H* index in a period from 0400 to 0800 UT, together with the large enhancement of the ΔH value at the daytime dip equator. The ΔH enhancement clearly suggests that the strong convection electric fields that lead to the eastward currents penetrate to the equatorial ionosphere in this period. On the other hand, the northward turning of the IMF causes the development of ring current to cease and leads to a larger depression of the ΔH value of TIR, compared with that of ABG. The significant depression of the ΔH value at the daytime dip equator clearly indicates that the reversed convection electric fields that lead to the westward currents penetrate to the equatorial ionosphere in this period. *AU* and *AL* show substorm signatures at 1600 UT during the later recovery phase of the magnetic storm on 31 March 2001. The local time at Indian stations is 0530 h ahead of UT.

[7] Figure 2 depicts a close-up view of 12 h of the data on 31 March, which shows the solar wind dynamic pressure

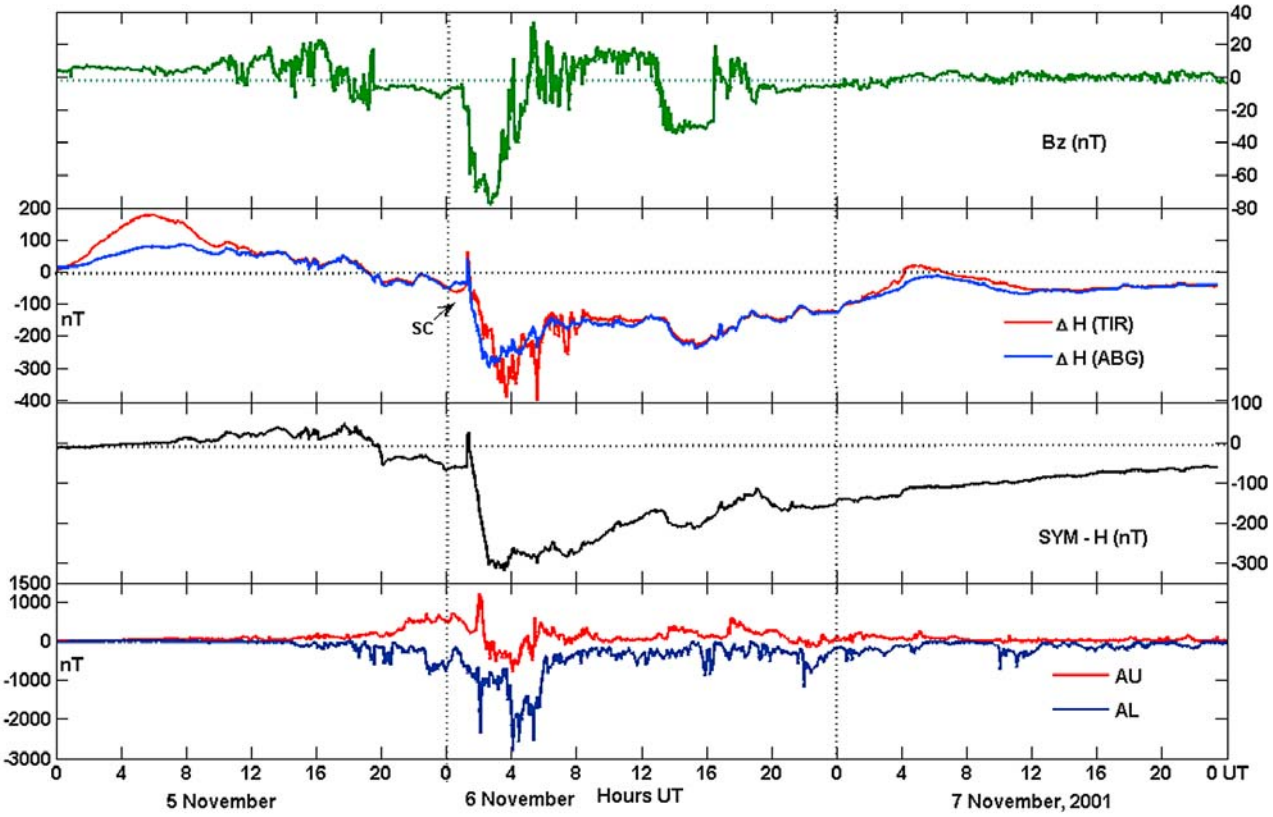

Figure 3. Magnetic storm of 6 November 2001 with ΔH of TIR and ABG, *SYM-H* index, interplanetary magnetic field component (IMF Bz) from ACE. The SC occurred at 0152 UT on 6 November 2001 accompanied with abrupt decrease in IMF Bz. The disturbed geomagnetic conditions (before SC) are seen in auroral eastward (*AL*) and westward electrojets (*AU*) at the nighttime of 5 November 2001. The local noon is at around 0600–0700 UT (1130–1230 LT), and local midnight is at around 1830–1930 UT (0000–0100 LT).

(Psw), IMF Bz, PCN index, calculated EEJ(Dis), and *SYM-H* index. At the time of SC, the dynamic pressure reached about 100 nPa, which is very high. After 0300 UT, the IMF Bz turned southward with a large amplitude of −45 nT and produced an extremely strong convection electric field in the inner magnetosphere during the main phase of the geomagnetic storm. This strong convection and the positive EEJ(Dis) seem to persist until the southward IMF Bz starts to decrease (~0700 UT). Here we focus on the two time intervals of 0230–0700 UT and 0700–0930 UT (which are marked by the thick vertical lines) in EEJ(Dis), which suggests the penetration of the two strong electric fields corresponding to the origin of the R1 and R2 FACs during the main and recovery phases of the geomagnetic storm, respectively. During the first interval, 0230–0700 UT (0800–1230 LT), the solar wind dynamic pressure shows large amplitude perturbations with an average magnitude of more than 20 nPa and IMF Bz also indicates a large oscillation in a range from 40 nT to −40 nT. These oscillations seem to manifest the fluctuations of the *DP* 2 currents originating from the R1 FACs. However, the time scale of the EEJ(Dis) fluctuations with magnitude of more than 180 nT does not match well with that of the IMF Bz variations. This implies that the *DP* 2 currents have a significant effect on the time variations of solar wind dynamic pressure and are also well correlated with the PCN index, which reflected as the strength of global convection. In the same period, a large enhancement of polar cap potential enhancement, identified from the DMSP-F13 satellite observations [*Hairston et al.*, 2003], takes place that leads to an intensification of the penetrating electric field for a longer period, in particular for 0400–0700 UT, as seen in the equatorial *DP* 2 currents (Figure 2). The second interval, 0700–0930 UT (1230–1500 LT), starts with the decrease of southward IMF Bz that led to the reversed convection electric field at the daytime equator as suggested by the CEJ occurrence at the beginning of the recovery phase. But at 0700 UT, EEJ(Dis) started to decrease, though IMF Bz is still southward, which shows that the shielding electric field is effective during the main phase and this condition persists for 1 h. Concurrently, the PCN drop exactly matches with decrease of EEJ(Dis) indicating the reduction of convection electric field. The appearance of CEJ with amplitude of ~−200 nT at local noon indicates the westward electric field at the equator that probably originated from R2 FACs. By examining the two intervals, the storm time EEJ(Dis) variations imply that the dawn-to-dusk and dusk-to-dawn electric fields play a dominant role in driving the eastward and westward electrojet during the main and recovery phases of the geomagnetic storm, respectively.

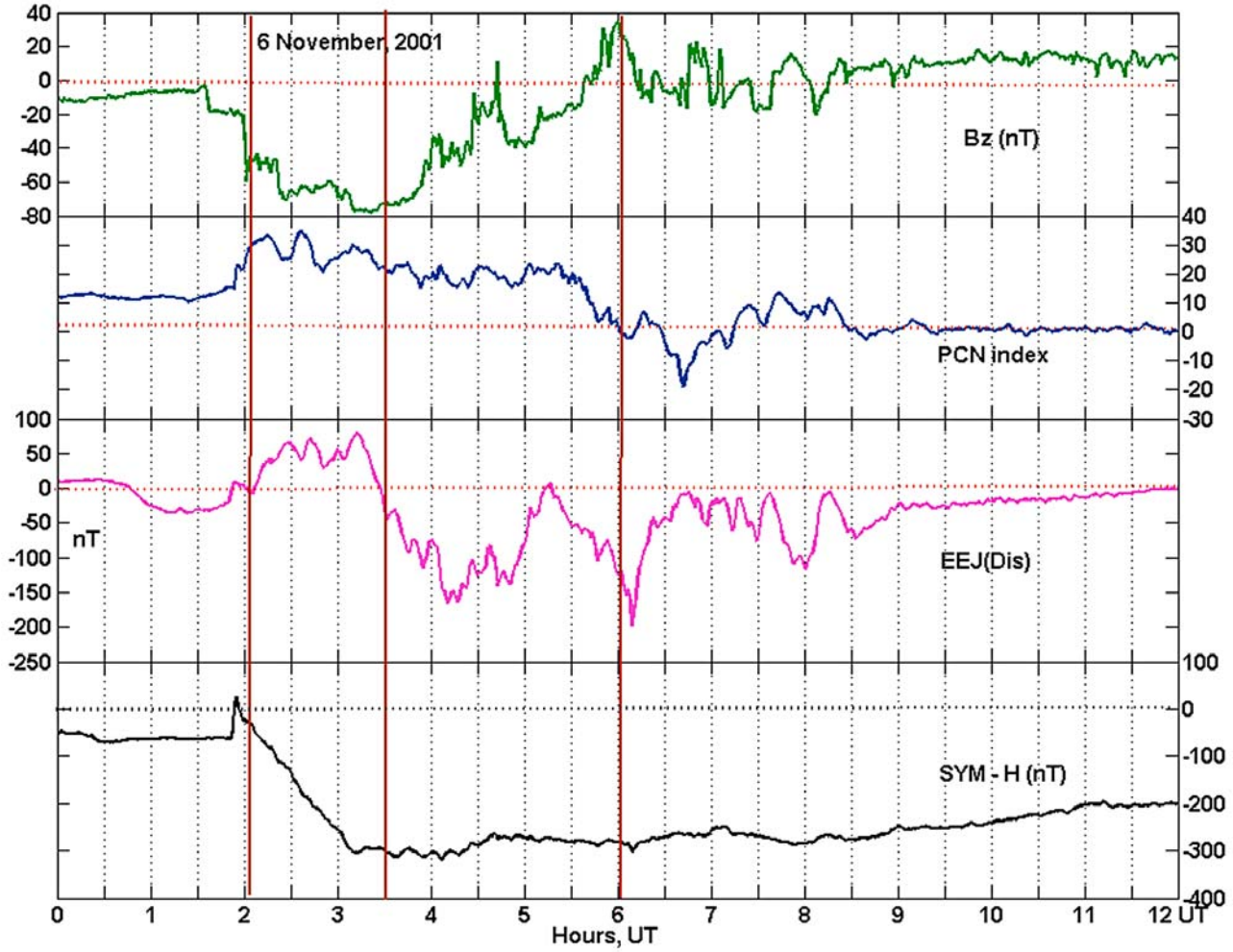

Figure 4. The storm time electrojet index, EEJ(Dis), along with *SYM-H*, PCN index, and IMF Bz for 6 November 2001 for the time interval of 0000–1200 UT. The local noon corresponds to 0600–0700 UT (1130–1230 LT). The portions between the thick vertical lines denote the variations of *DP* 2 currents at the equator and CEJ during the main phase and recovery phases of the magnetic storm of 6 November 2001.

3.2. Geomagnetic Storm on 6 November 2001

[8] Figure 3 presents the second intense magnetic storm event on 6 November 2001 in the same format as in Figure 1, and IMF data (Bz) are time-shifted about 35 min. This storm was driven by the CME phenomena generated by major solar flare eruption at 1620 UT on 4 November 2001. The solar flare caused a strong solar radiation storm and proton event. After about 33 h, the interplanetary shock associated with the CME impacted the Earth's magnetosphere. Because of the arrival of the interplanetary shock, the SC phenomenon is seen in low and equatorial magnetograms at 0150 UT on 6 November. Although the ACE and Wind satellite data were not available, SOHO/CELIAS could detect the impact shock and reported a steep increase in velocity from 450 to 720 km/s at 0115 UT on 6 November 2001, and the compressional effect of this shock was seen as a two-step density enhancement at 0115 and 0155 UT [*Alex et al.*, 2005]. Before the onset of SC, the ΔH of TIR and ABG are in the negative because of development of ring current (negative *SYM-H*) with southward IMF Bz, indicating the disturbed conditions of a proton event that are noted in *AU* and *AL* indices during the night of 5 November. After the onset of SC, the main phase started immediately, and the ring current is abruptly enhanced because of the strong IMF Bz of −70 nT. During the main phase, the ΔH plots of TIR and ABG show a steep decrease of −384 nT at around 0400 UT (0930 LT) and −295 nT at around 0300 UT (0830 LT), respectively. The excess decrease in the ΔH value of TIR as compared with *SYM-H* indicates a clear signature of ionospheric *DP* 2 currents superposed on the ring current effects that appear dominantly at ABG. The negative value of the *AU* index at 0300 UT on 6 November indicates the equatorward expansion of auroral oval due to enhanced convection because of large southward IMF.

[9] Figure 4 presents a close-up view of the 6 November magnetic storm in the same format as Figure 3 without the solar wind dynamic pressure because of nonavailability of data. We focus on two intervals (marked by thick vertical lines),

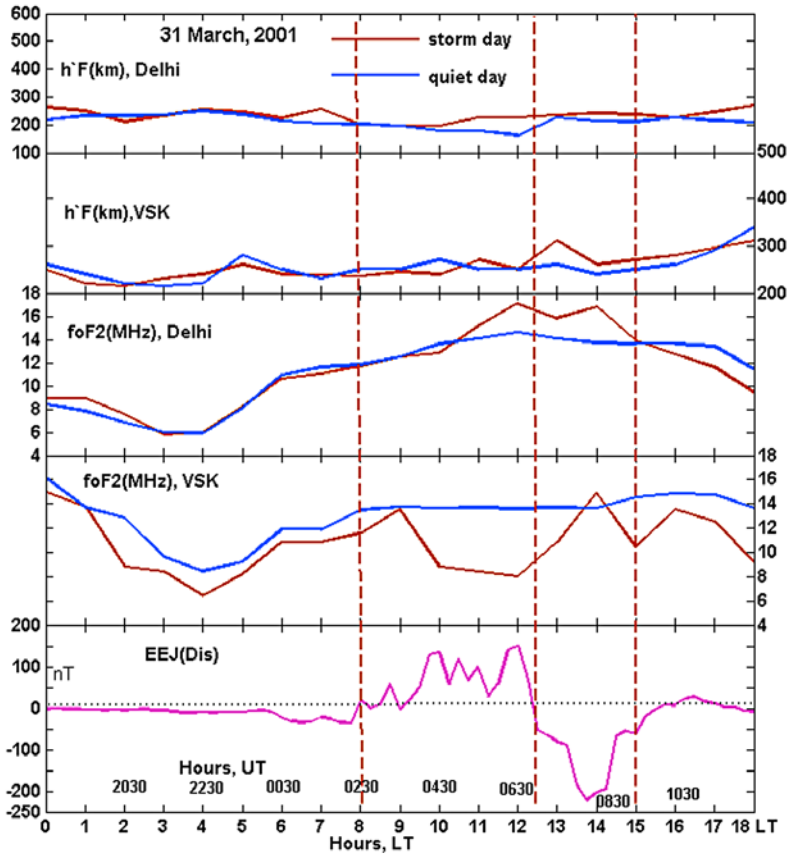

Figure 5. Low-latitude ionospheric *F* region response to the severe magnetic storm of 31 March 2001. During the main phase, the higher amplitudes in EEJ(Dis) due to the strong eastward electric field at the equator caused the decrease in critical frequencies (f_oF_2) at Vishakhapatnam (VSK), indicating the enhancement of EIA on 31 March 2001 when compared with quiet day (see text). The time interval is given in LT, and the corresponding UT is also shown on the *X* axis.

0200–0330 UT and 0330–0610 UT, which clearly indicate the changes in electric fields. The daytime variations of *DP* 2 currents are clearly seen in EEJ(Dis) with a large amplitude of 97 nT at around 0310 UT (0840 LT), which coincides with the maximum southward IMF Bz with a value of −78 nT. In this case, the magnitude of EEJ(Dis) is smaller than that of the previous storm event in spite of strong southward IMF Bz. The amplitude difference of EEJ(Dis) between two storm events (mentioned in this study) indicates a local time dependence of the EEJ(Dis) strength. The TIR station was located around noon for the March 31 storm event, while the station was located in the morning sector of 0830 LT with insufficient ionospheric conductivity for this event. On the other hand, associated with the start of the reduction of the southward IMF Bz intensity, the EEJ(Dis) variations show an abruptly negative excursion with a peak magnitude of −150 nT around 0410 UT (0940 LT). This signature indicates an appearance of CEJ driven by the westward electric field originating from the R2 FACs despite the southward IMF Bz with magnitude of −40 nT. The occurrence of CEJ, during the period 0330–0610 UT (0900–1140 LT), corresponds to the reduction of southward IMF Bz intensity (second interval, marked by thick vertical lines). In between this second interval, CEJ starts to recover (or decrease) with increase of southward IMF Bz at 0445 UT and again strengthen after 0515 UT with northward turning of IMF Bz. After 0310 UT, the abrupt decrease of EEJ(Dis) exactly coincides with the decrease of polar cap potential index (PCN) during the main phase, in spite of IMF Bz southward, which indicates the dominance of shielding electric field due to R2 FACs, and this situation persists for 1 h. Therefore, a significant overshielding effect tends to appear in the case of the reduction of the convection electric field originating from the R1 FACs. Therefore, when the R1 FACs and polar cap potential decreased considerably, CEJ tends to appear at the daytime equator. The overshielding effect persists for 3 h at the beginning of recovery phase.

3.3. Equatorial and Low-Latitude Ionospheric Response to Geomagnetic Storms

[10] In this section, we analyze ionosonde data from a chain of the Indian stations to examine how the low-latitude and equatorial *F* region plasmas respond to the enhanced EEJ/CEJ conditions due to the penetrating electric fields. We also try to explore possible reasons for the enhancement/inhibition of EIA. Figure 5 shows the response of the ionospheric *F* region plasmas in the equatorial and low-latitude regions during the geomagnetic storm on 31 March 2001 for

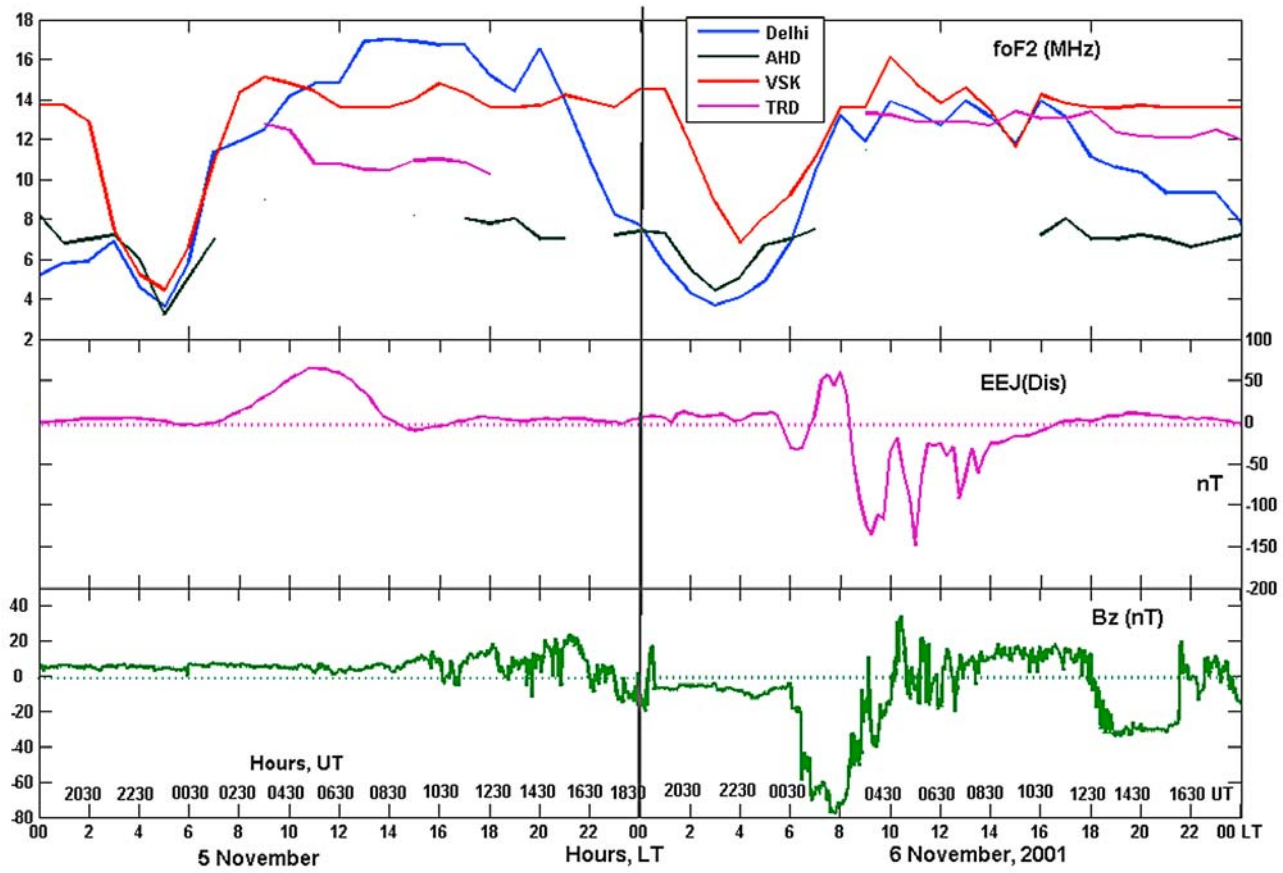

Figure 6. Low-latitude ionospheric *F* region response to the severe magnetic storm of 6 November 2001. During the recovery phase, at local noon, the strong CEJ due to westward electric fields at the equator altered the critical frequencies at all the stations. The inhibition of EIA is clearly seen on 6 November as compared to normal EIA on 5 November due to the effect of CEJ. The time interval is given in LT, and the corresponding UT is also shown on the *X* axis.

the time interval 0000–1800 LT. The first through fourth panels of Figure 5 give a comparison of ionospheric parameters of the *F* region, f_oF_2 (maximum critical frequency) and $h'F$ (minimum virtual height), at Delhi and Vishakahapatnam (VSK) between the quiet and storm periods indicated by the blue and red lines, respectively. In the present analysis, we used the averaged values for 5 quiet days obtained from VSK and Delhi shown by blue lines. The EEJ(Dis) data are averaged for 15 min to agree with the time resolution of the ionospheric data. In Figure 5 (fifth panel), it is shown that the two time intervals of 0230–0700 UT (0800–1230 LT) and 0700–0930 UT (1230–1500 LT) (marked by vertical dashed lines) represent strong enhancements in EEJ and CEJ (as in Figure 2), respectively. The $f_oF_2$value at the equatorial station VSK shows a large decrease from the quiet value of about 14 MHz to about 6.5 MHz after a significant enhancement of the EEJ(Dis) (1000–1200 LT). The low-latitude station Delhi shows no significant simultaneous change in f_oF_2 compared with the quiet time level, indicating that the crest of the strong EIA might have formed beyond the latitude of Delhi. The second interval (1230–1500 LT) represents the strong CEJ, during this period the f_oF_2 started to increase at VSK as the effect of reversed electric field, i.e., westward electric field. It should be noted that although there is not much change in the $h'F$ value, the height of h_mF_2 (maximum height of the F_2 layer) rises about 150 km compared with quiet day at VSK (K. Niranjan, private communication, 2008) and almost no change of h_mF_2 in Delhi. The depletion of f_oF_2 at VSK and rise of f_oF_2 at Delhi could be due to a strong EIA enhancement associated with a super plasma fountain effect. Therefore, the plasma depletion can be extended to away from equator due to the above physical processes. The *F* region response in the second interval shows a sudden increase in f_oF_2 by about 8 MHz at VSK and a drop of 2 MHz at Delhi, which seems to indicate a reduction or inhibition of equatorial ionization anomaly (EIA), corresponding to an appearance of strong CEJ, i.e., westward electric field in the daytime equator.

[11] Similarly, the ionospheric *F* region response during the intense magnetic storm on 6 November 2001 is presented in Figure 6 using the ionosonde data from a chain of stations distributed from the dip equator to low latitudes. The time interval is 2 days from 5–6 November 2001. The normal EEJ strength of about 70 nT is noted on 5 November with well developed EIA. The f_oF_2 shows a considerable difference from the equator to low-latitude stations with

lowest f_oF_2 at 1300 LT (9.5 MHz) at TRD, high f_oF_2 at VSK (13.5 MHz), and highest f_oF_2 at Delhi (17.6 MHz) on 5 November, indicating a well-developed noontime EIA as plasma moves from the equator to low latitudes. Compared with the quiet day on 5 November 2001, f_oF_2 undergoes significant changes during the storm day on 6 November. The diurnal profile of the electrojet strength showed a considerable distortion due to noontime strong CEJ on 6 November because of reversed electric fields. Although the large enhancement of EEJ strength with 70 nT at 0730 LT (6 November) associated with the strong southward IMF Bz indicates the penetration of a strong eastward electric field (Figure 6), there was a time delay between the EEJ enhancement and the formation of ionization anomaly, and 0730 LT is too early for the development of EIA. But the plasma distribution is completely altered by the effect of strong CEJ (~−150 nT) due to westward electric fields for the period 0900–1400 LT. This condition continued for 4 h with associated changes in IMF Bz. On 6 November at 1000 LT, the increase in the f_oF_2 values for TRD (4 MHz), and VSK (2.5 MHz) and the decrease in the f_oF_2 value at Delhi (3 MHz) compared with that of 5 November values indicate the poor development of EIA (as plasma is not transported from equator to low latitudes) with a small change in $h'F$ but a 200 km (not shown) rise in h_mF_2 at TRD and 65 km at Delhi (K. Niranjan, private communication, 2008). It is also observed that there is no large difference in f_oF_2 values at all three stations during noontime on 6 November because of a large CEJ interval. These results clearly confirm the reduction or inhibition of EIA due to the strong CEJ during the local noontime, and the plasma response time being less than 30 min in response to ionospheric electric fields.

4. Discussion

[12] We have observed that amplitude enhancements of *DP* 2 currents and strong CEJ due to enhancement of eastward/westward electric fields during the main and recovery phases of the magnetic storm are possibly due to prompt penetration of electric fields from high latitudes. In this section, we will discuss the character of enhancement of convection electric fields and their implications on the equatorial and low-latitude ionosphere. The equatorial *DP* 2 current system, which is driven by the convection electric field originating from the polar region, expanded instantaneously to the equatorial latitudes because of the arrival of strong southward IMF Bz during the main phase of the geomagnetic storms, as suggested by *Kikuchi et al.* [2008]. The *DP* 2 currents driven by the eastward electric field were more effective on the equatorial ionosphere in the dusk sector than those in the daytime sector [*Abdu et al.*, 1998]. However, during the main phase of the geomagnetic storm on 31 March 2001, the eastward electric field was enhanced significantly in the entire region from morning to noon sectors, i.e., during 0330–0700 UT (0900–1230 LT) (Figure 2). Simultaneously, the polar cap potential drop reached up to 350 kV, on the basis of the model calculations and also the DMSP-F13 satellite observations [*Hairston et al.*, 2003]. Therefore, the strong convection electric fields and R1 FACs generated because of the southward IMF Bz (−30 to −46 nT) lead to an intensification of the *DP* 2 current system connected to the equatorial Pedersen currents, which produce a large amplitude of EEJ(Dis) reaching up to 200 nT at the daytime equator (Figure 2). A few minutes after the increase of PCP and *DP* 2 currents due to the southward turning of IMF Bz, the asymmetric ring current develops in the inner magnetosphere, which leads to a large depression of geomagnetic field on the ground [*Hashimoto et al.*, 2002]. The increase in EEJ(Dis) with simultaneous increase of PCN is in very good agreement with the results of *Kikuchi et al.* [2008]. The decrease in TIR-ABG variation (Figure 1) may be due to overshielding that was led by reduction of the R1 field-aligned currents. For the same event, the disturbance dynamo was not dominant during the large enhancement of eastward electric field in the daytime sector as reported by *Maruyama et al.* [2005] using RCM and CTIP models.

[13] At the onset of the recovery phase associated with the decrease of southward IMF Bz at 0700 UT (Figure 2), the dawn-to-dusk electric field and R1 FACs suddenly weaken within a few minutes, and the dusk-to-dawn electric field originating from R2 FACs is dominant in the middle and equatorial ionosphere (the so-called overshielding state). The penetration of the dusk-to-dawn electric field to the equator led to the strong CEJ with the amplitude of −200 nT in the daytime sector (Figure 2). This condition persisted for 2 h up to 0930 UT. During the main phase, it is noticed that when the convection electric field started to decrease despite the southward IMF Bz condition, the shielding electric field penetrated to the equator for 1 h (0700–0800 UT). After that, the IMF Bz changes to northward and the electric field reversed with a larger amplitude from eastward to westward direction at the daytime equator because of the dominating shielding effect [*Kelley et al.*, 1979], and a sudden change in the polar cap potential could produce this dramatic change in the direction of equatorial electric fields [*Peymirat et al.*, 2000]. *Kikuchi et al.* [2003] observed CEJ at the afternoon dip equator during the recovery phase of the substorm and attributed it to fully developed R2 FACs, when R1 FACs decrease suddenly with an abrupt decrease of PCP [*Kikuchi et al.*, 2000].

[14] Also, in the case of the 6 November magnetic storm (Figure 4), a remarkable enhancement of the EEJ(Dis) at 0200–0330 UT (0730–0900 LT) during the main phase is consistent with the results of *Kikuchi et al.* [2008] and *Huang et al.* [2005]. This magnetic storm has been investigated using the equatorial station Yap (YAP, −0.3° GML) and the low-latitude station Okinawa (OKI, 14.47° GML) from Japan's sector, and it has been shown that the strong EEJ (YAP–OKI) enhancement with an amplitude of 250 nT is observed at 0200 UT (1100 LT) and CEJ with a minimum value of −170 nT at 0430 UT (1330 LT) [*Kikuchi et al.*, 2008]. However, in spite of the large southward IMF Bz (−78 nT) period, the maximum amplitude (70 nT) of EEJ (Dis) during the interval of 0200–0330 UT is much smaller than that reported by *Kikuchi et al.* [2008], and the difference between the amplitude enhancements of EEJ and CEJ in both sectors seems to be due to the longitudinal dependence of ionospheric conductivity (varies with local time) [*Tsunomura*, 1999]. However, in this study, it is shown that the second CEJ was most enhanced with a maximum amplitude of −193 nT at 0610 UT (1140 LT), although the CEJ amplitude in the Japan sector was less than half of the amplitude observed in the Indian sector. It is also noted that

the strong one-to-one correlation between EEJ(Dis) and IMF Bz (Figure 4) implies the dominance of penetrating electric fields rather than the disturbance dynamo. Furthermore, the enhanced shielding electric field tended to appear in the daytime sector at the equator with correspondence to the weakness of the southward IMF Bz or northward turning of the IMF Bz. This signature of the CEJ appearance indicates that the shielding electric field originating from the R2 FACs tends to be more dominant when the convection electric field originating from the R1 FACs suddenly weakens, which is associated with an abrupt decrease of the magnitude of the southward IMF Bz. These facts support the results of previous theories [*Senior and Blanc*, 1984; *Peymirat et al.*, 2000] and empirical models [*Fejer and Scherliess*, 1995; *Fejer et al.*, 2007], but we need to take into account the local time dependence of the ionospheric conditions.

[15] *Huang et al.* [2005] showed the long duration of penetrating electric fields to the low-latitude ionosphere without the significant effects of the shielding electric field during the main phase of the geomagnetic storms under the condition that the IMF Bz remains in the southward direction for a long time, from 2 to 4 hours, by analyzing a few magnetic storm with *Dst* between −50 and −100 nT. However, the present analysis shows that the amplitude of the EEJ(Dis) produced by the dawn-to-dusk electric field originating from the R1 FACs tends to decrease during the course of the development of the ring current in the inner magnetosphere during the main phase of the two intense geomagnetic storms. This tendency suggests that the shielding electric field grows together with the development of the R2 FACs connected to the partial ring current and becomes effective during the late main phase. Therefore, from this signature of the storm time EEJ(Dis), it can be concluded that the shielding effect at the equator is determined by the competition between the magnitude of the R1 FACs and the R2 FACs. This interpretation supports the theory of *Kikuchi et al.* [2008] and is consistent with the observational fact that the eastward electric field is not always proportional to the solar wind electric field and the polar cap potential drop reported by *Fejer et al.* [2007]. But our observations clearly indicate that during the main phase of intense magnetic storms, penetration of shielding electric field to the equator lasts approximately 1 h with steady IMF Bz southward but not several hours because of the development of the overshielding effect with IMF Bz turning northward or a decrease in southward IMF Bz, which causes strong CEJ at equator. At this time, the ring current intensity is maximum and steady for 1 h, and it is a transition time for changing from the main phase to the recovery phase (Figures 2 and 4). In the future, we need to investigate other severe magnetic storms with intensified steady ring current for several hours with simultaneous changes in penetrating electric fields and associated shielding conditions.

[16] The penetrating electric field causes significant disturbances in the low-latitude ionosphere at the daytime and nighttime sectors and modifies the *F* region plasma density and its layer heights during the main and recovery phases of geomagnetic storms. When the IMF Bz turns southward, the strong eastward electric fields penetrate to the equator and lead to uplift ionospheric plasma at around 10° GML across the equator, which is called a strong positive ionospheric storm. This super fountain effect also shifts the EIA crests to higher latitudes, and the region of ionospheric plasma depletion can be extended to higher than normal latitudes. During the main phase on 31 March 2001, the strong eastward electric field led to the enhancement of the EEJ around noon and caused the strong EIA enhancement and plasma depletion observed at Visakapatnam (8.34° GML). This is consistent with model results of the super plasma fountain and its effects on EIA [*Balan et al.*, 2009]. However, modeling studies later showed that though the eastward penetration electric field reduces electron density (Nmax) or f_oF_2 (and total electron content) around the equator (through super fountain) as shown by the ionospheric data (Figures 5 and 6), an equatorward neutral wind is required to enhance the density at and beyond the equatorial anomaly crests. This has been shown using coupled ionosphere-thermosphere and ionosphere-plasmasphere models and confirmed by observations [e.g., *Lin et al.*, 2005; *Vijaya Lekshmi et al.*, 2007; *Lu et al.*, 2008].

5. Conclusions

[17] The study of two intense magnetic storms provides us with the complex electrodynamics that can be useful for the understanding of existing theories. By analyzing the geomagnetic field variations of the *H* component obtained from TIR and ABG, the storm time electrojet index, EEJ(Dis), in conjunction with IMF Bz strength and ionosonde measurements at equatorial latitudes, showed some outstanding features of the penetrating electric fields and their implications on the low-latitude ionosphere.

[18] 1. During the main phase of the magnetic storm, the penetration of the strong convection electric fields to the equator lasts for 2 h in the daytime sector, corresponding to the period of large polar cap potential drops. The magnitude of the equatorial ionospheric currents driven by the penetrating electric fields is very sensitive to the ionospheric conductivity (which depends on local time).

[19] 2. The time delay for the response of *DP* 2 currents to the development of ring current during the onset time of geomagnetic storms depends on the local time and phase of the storm.

[20] 3. The convection electric field started to decrease for an hour from the start time of the main phase in spite of the significant southward IMF Bz. This phenomenon can be interpreted in terms of the shielding electric field being effective during the late main phase associated with the growth of the partial ring current in the inner magnetosphere, which is connected to the R2 FACs.

[21] 4. During intense geomagnetic storms, the penetrating electric fields from high latitudes cause the strong EEJ and CEJ at the equator, leading to changes in *F* region ionospheric plasma densities like enhanced EIA during the main phase and EIA inhibition/reduction during the recovery phase, respectively. These signatures are evidently seen in EEJ(Dis).

[22] **Acknowledgments.** Part of this work was supported by the Grant-in-Aid for Nagoya University Global COE Program "Quest for Fundamental Principles in the Universe: From Particles to the Solar System and the Cosmos" from the Ministry of Education, Culture, Sports, Science and Technology of Japan. We thank the World Data Center for

Geomagnetism, Kyoto, for *Dst* index and the ACE SWEPAM instrument team, MAG instrument team, and the ACE science center for ACE solar wind data. We also thank the National Physical Laboratory, New Delhi, and Andhra University, Visakapatnam, for providing the ionospheric data. Special thanks to Yuji Tsuji and Y. Ebihara for useful discussions.

[23] Wolfgang Baumjohann thanks the reviewers for their assistance in evaluating this paper.

References

Abdu, M. A., J. H. Sastri, H. Luhr, H. Tachihara, T. Kitamura, N. B. Trivedi, and J. H. A. Sobral (1998), *DP* 2 electric field fluctuations in the duskside dip equatorial ionosphere, *Geophys. Res. Lett.*, *25*, 1511–1514.

Alex, S., A. Patil, and R. G. Rastogi (1986), Equatorial counter electrojet—Solution of some dilemma, *Indian J. Radio Space Phys.*, *15*, 114–118.

Alex, S., B. M. Pathan, and G. S. Lakhina (2005), Response of low latitude geomagnetic field to the major proton event of November 2001, *Adv. Space Res.*, *36*, 2434–2439.

Balan, N., K. Shiokawa, Y. Otsuka, S. Watanabe, and G. Bailey (2009), Super plasma fountain ionization anomaly during penetration electric fields, *J. Geophys. Res.*, *114*, A03310, doi:10.1029/2008JA013768.

Blanc, M., and A. D. Richmond (1980), The ionospheric disturbance dynamo, *J. Geophys. Res.*, *85*(A4), 1669–1686.

Dungey, J. W. (1961), Interplanetary magnetic field and auroral zones, *Phys. Res. Lett.*, *6*, 47–48.

Fang, T. W., A. D. Richmond, J. Y. Liu, and A. Maute (2008), Wind dynamo effects on ground magnetic perturbations and vertical drifts, *J. Geophys. Res.*, *113*, A11313, doi:10.1029/2008JA013513.

Fejer, B. G. (2002), Low latitude storm time ionospheric electrodynamics, *J. Atmos. Sol. Terr. Phys.*, *64*, 1401–1408.

Fejer, B. G., and L. Scherliess (1995), Time-dependent response of equatorial ionospheric electric fields to magnetic disturbances, *Geophys. Res. Lett.*, *22*, 851–854.

Fejer, B. G., J. W. Jensen, T. Kikuchi, M. A. Abdu, and J. L. Chau (2007), Equatorial ionospheric electric fields during the November 2004 magnetic storm, *J. Geophys. Res.*, *112*, A10304, doi:10.1029/2007JA012376.

Gonzales, C. A., M. C. Kelley, B. G. Fejer, J. F. Vickrey, and R. F. Woodman (1979), Equatorial electric fields during magnetically disturbed conditions: 2. Implications of simultaneous auroral and equatorial measurements, *J. Geophys. Res.*, *84*, 5803–5812.

Hairston, M. R., T. W. Hill, and R. A. Heelis (2003), Observed saturation of the ionospheric potential during the 31 March 2001 storm, *Geophys. Res. Lett.*, *30*(6), 1325, doi:10.1029/2002GL015894.

Hanson, W. B., and R. J. Moffett (1966), Ionization transport effects in the equatorial *F* region, *J. Geophys. Res.*, *71*, 5559–5572.

Hashimoto, K. K., T. Kikuchi, and Y. Ebihara (2002), Response of the magnetospheric convection to sudden interplanetary magnetic field changes as deduced from the evolution of partial ring currents, *J. Geophys. Res.*, *107*(A11), 1337, doi:10.1029/2001JA009228.

Huang, C.-S., J. C. Foster, and J. M. Holt (2001), Westward plasma drift in the midlatitude ionospheric *F* region in the midnight-dawn sector, *J. Geophys. Res.*, *106*(A12), 30,349–30,362.

Huang, C.-S., J. C. Foster, and M. C. Kelley (2005), Long-duration penetration of the interplanetary electric field to the low-latitude ionosphere during the main phase of magnetic storms, *J. Geophys. Res.*, *110*, A11309, doi:10.1029/2005JA011202.

Jaggi, R. K., and R. A. Wolf (1973), Self-consistent calculation of the motion of a sheet of ions in the magnetosphere, *J. Geophys. Res.*, *78*(16), 2852–2866.

Kelley, M. C., B. G. Fejer, and C. A. Gonzales (1979), An explanation for anomalous equatorial ionospheric electric field associated with a northward turning of the interplanetary magnetic field, *Geophys. Res. Lett.*, *6*, 301–304.

Kelley, M. C., M. N. Vlasov, J. C. Foster, and A. J. Coster (2004), A quantitative explanation for the phenomenon known as storm-enhanced density, *Geophys. Res. Lett.*, *31*, L19809, doi:10.1029/2004GL020875.

Kikuchi, T., and T. Araki (1979), Horizontal transmission of the polar electric field to the equator, *J. Atmos. Sol. Terr. Phys.*, *41*, 927–936.

Kikuchi, T., T. Araki, H. Maeda, and K. Maekawa (1978), Transmission of polar electric fields to the equator, *Nature*, *273*, 650–651.

Kikuchi, T., H. Luehr, T. Kitamura, O. Saka, and K. Schlegel (1996), Direct penetration of the polar electric field to the equator during a *DP* 2 event as detected by the auroral and equatorial magnetometer chains and the EISCAT radar, *J. Geophys. Res.*, *101*(A8), 17,161–17,173.

Kikuchi, T., H. Luehr, K. Schlegel, H. Tachihara, M. Shinohara, and T.-I. Kitamura (2000), Penetration of auroral electric fields to the equator during a substorm, *J. Geophys. Res.*, *105*(A10), 23,251–23,261.

Kikuchi, T., K. K. Hashimoto, T.-I. Kitamura, H. Tachihara, and B. Fejer (2003), Equatorial counterelectrojets during substorms, *J. Geophys. Res.*, *108*(A11), 1406, doi:10.1029/2003JA009915.

Kikuchi, T., K. Hashimoto, and K. Nozaki (2008), Penetration electric fields to the equator during a geomagnetic storm, *J. Geophys. Res.*, *113*, A06214, doi:10.1029/2007JA012628.

Kobea, A. T., A. D. Richmond, B. A. Emery, C. Peymirat, H. Luehr, T. Moretto, M. Hairston, and C. Amory-Mazaudier (2000), Electrodynamic coupling of high and low latitudes: Observations on May 27, 1993, *J. Geophys. Res.*, *105*(A10), 22,979–22,989.

Lin, C. H., A. D. Richmond, R. A. Heelis, G. J. Bailey, G. Lu, J. Y. Liu, H. C. Yeh, and S.-Y. Su (2005), Theoretical study of the low- and mid-latitude ionospheric electron density enhancement during the October 2003 superstorm: Relative importance of the neutral wind and the electric field, *J. Geophys. Res.*, *110*, A12312, doi:10.1029/2005JA011304.

Lu, G., L. P. Goncharenko, A. D. Richmond, R. G. Roble, and N. Aponte (2008), A dayside ionospheric positive storm phase driven by neutral winds, *J. Geophys. Res.*, *113*, A08304, doi:10.1029/2007JA012895.

Maruyama, N., A. D. Richmond, T. J. Fuller-Rowell, M. V. Codrescu, S. Sazykin, F. R. Toffoletto, R. W. Spiro, and G. H. Millward (2005), Interaction between direct penetration and disturbance dynamo electric fields in the storm-time equatorial ionosphere, *Geophys. Res. Lett.*, *32*, L17105, doi:10.1029/2005GL023763.

Nishida, A. (1968), Coherence of *DP* 2 fluctuations with interplanetary magnetic field variations, *J. Geophys. Res.*, *73*, 5549–5559.

Nishida, A., N. Iwasaki, and T. Nagata (1966), The origin of fluctuations in the equatorial electrojet: A new type of geomagnetic variation, *Ann. Geophys.*, *22*, 478–484.

Peymirat, C., A. D. Richmond, and A. T. Kobea (2000), Electrodynamic coupling of high and low latitudes: Simulations of shielding/overshielding effects, *J. Geophys. Res.*, *105*(A10), 22,991–23,003.

Rastogi, R. G. (2004), Westward electric field in the low latitude ionosphere during the main phase of magnetic storms occurring around local midday hours, *Sci. Lett.*, *27*, 69–74.

Rastogi, R. G., and V. L. Patel (1975), Effect of interplanetary magnetic field on ionosphere over the magnetic equator, *Proc. Indian Acad. Sci.*, *82*, 121–141.

Reddy, C. A., V. V. Somayajulu, and C. V. Devasia (1979), Global scale electrodynamic coupling of the auroral and equatorial dynamo regions, *J. Atmos. Terr. Phys.*, *41*, 189–201.

Reddy, C. A., V. V. Somayajulu, and K. S. Viswanathan (1981), Backscatter radar measurements of storm-time electric field changes in the equatorial electrojet, *J. Atmos. Terr. Phys.*, *43*, 817–827.

Senior, C., and M. Blanc (1984), On the control of magnetospheric convection by the spatial distribution of ionospheric conductivities, *J. Geophys. Res.*, *89*(A1), 261–284.

Somayajulu, V. V., C. A. Reddy, and K. S. Viswanathan (1987), Penetration of magnetospheric convective electric field to the equatorial ionosphere during the substorm of March 22, 1979, *Geophys. Res. Lett.*, *14*(8), 876–879.

Southwood, D. J. (1977), The role of hot plasma in magnetospheric convection, *J. Geophys. Res.*, *82*(35), 5512–5520.

Srivastava, N., and P. Venkatakrishnan (2002), Relationship between CME speed and geomagnetic storm intensity, *Geophys. Res. Lett.*, *29*(9), 1287, doi:10.1029/2001GL013597.

Tsunomura, S. (1999), Numerical analysis of global ionospheric current system including the effect of equatorial enhancement, *Ann. Geophys.*, *17*, 692–706.

Tsurutani, B., et al. (2004), Global dayside ionospheric uplift and enhancement associated with interplanetary electric fields, *J. Geophys. Res.*, *109*, A08302, doi:10.1029/2003JA010342.

Tsurutani, B. T., et al. (2008), Prompt penetration electric fields (PPEFs) and their ionospheric effects during the great magnetic storm of 30–31 October 2003, *J. Geophys. Res.*, *113*, A05311, doi:10.1029/2007JA012879.

Vasyliunas, V. M. (1972), The interrelationship of magnetospheric processes, in *Earth's Magnetospheric Processes*, edited by B. M. McCormac, pp. 29–38, D. Reidel, Norwell, Mass.

Veenadhari, B., and S. Alex (2006), Space weather effects on low latitude geomagnetic field and ionospheric plasma response, in *Solar Influence on the Heliosphere and Earth's Environment: Recent Progress and Prospects*, edited by N. Gopalswamy and A. Bhattacharyya, pp. 395–398, Quest, Mumbai.

Vijaya Lekshmi, D., N. Balan, V. K. Vaidyan, H. Alleyne, and G. J. Bailey (2007), Response of the ionosphere to super geomagnetic storms: Observations and modeling, *Adv. Space Res.*, *41*, 548–555, doi:10.1016/j.asr.2007.08.029.

Wilson, G. R., W. J. Burke, N. C. Maynard, C. Y. Huang, and H. J. Singer (2001), Global electrodynamics observed during the initial and main phases of the July 1991 magnetic storm, *J. Geophys. Res.*, *106*(A11), 24,517–24,539.

Wygant, J., D. Rowland, H. J. Singer, M. Temerin, F. Mozer, and M. K. Hudson (1998), Experimental evidence on the role of the large spatial scale electric field in creating the ring current, *J. Geophys. Res.*, *103*(A12), 29,527–29,544.

S. Alex, R. Singh, and B. Veenadhari, Indian Institute of Geomagnetism, Kalamboli Highway, New Panvel, Navi Mumbai 410218, India. (bveena@iigs.iigm.res.in)

E. Chandrasekhar, Department of Earth Sciences, Indian Institute of Technology, Powai, Mumbai 400076, India.

T. Kikuchi and A. Shinbori, Solar-Terrestrial Environment Laboratory, Nagoya University, Furo-cho, Chikusa-ku, Nagoya, 464-8601, Japan.